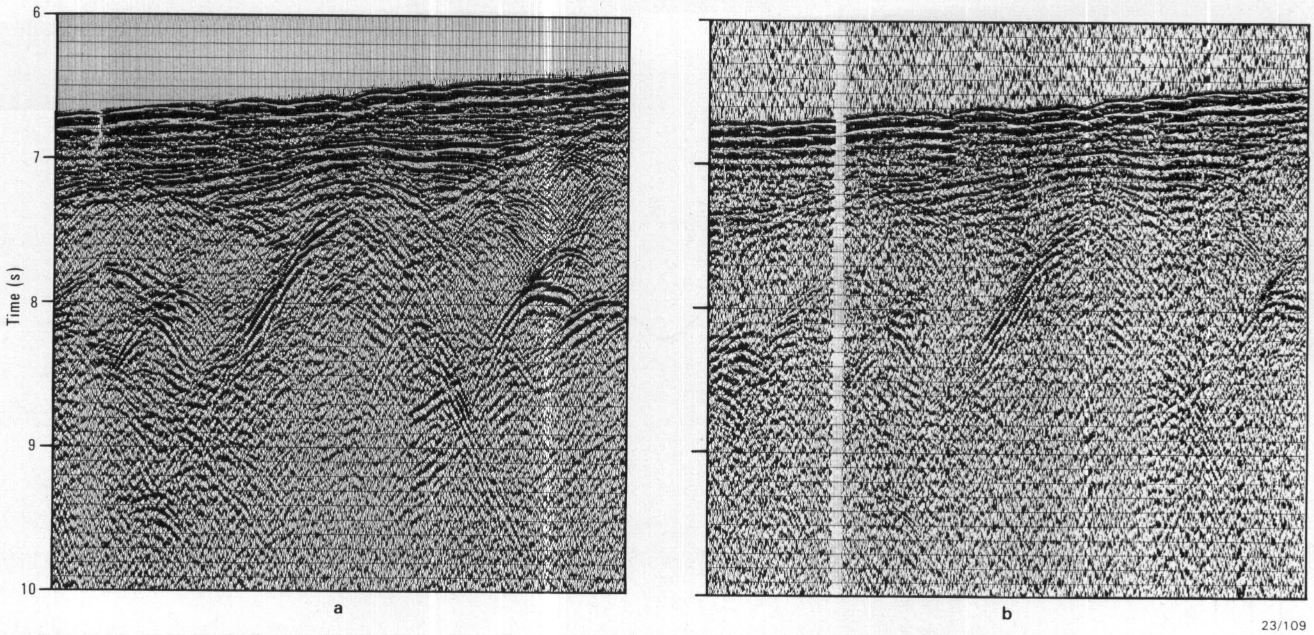

FIGURE 4
(a) Processed Deep Water Section.
(b) Near Trace Deep Water Section.

Terrace-function inversion for three-dimensional modelling of potential-field data

Lindrith Cordell

U.S. Geological Survey
P.O. Box 25046, Federal Centre MS964
Denver, Colorado 80225, USA

Summary

A recursive operator based on evaluation of the sense of local curvature, named the 'terracing operator', transforms smoothly varying potential-field data into a step function, consisting of steeps and flats. The terraced function, rescaled to units of physical property, provides a first approximation for data inversion from which a satisfactory final solution is quickly derived. The method is directly applicable to gravity data and can be applied to aeromagnetic data that have been transformed to pseudo-gravity. The objectives of the method are somewhat akin to those of susceptibility mapping, but differ in that the terraced function, like a geologic map, favours uniform physical property domains with sharp domain boundaries. It suppresses both ringing at the boundaries due to Gibbs' phenomenon (an advantage) and gradational physical property variation (possibly a disadvantage).

Introduction

Regional gravity and aeromagnetic maps are often perceived as out-of-focus geologic maps — with lithologic contacts present but blurred by the inherent lack of abrupt steps and discontinuities in the potentional-field data. A geologic map traditionally comprises uniform domains bounded by sharp, hard-edged boundaries and reflects a tacit assumption that the essential physical property functions are constant within domains and that their deivatives are undefined at domain boundaries. The associated potential-field functions, by contrast, vary within domains and (by definition) lack discontinuities in their derivatives.

Geologic map-like physical-property step functions and their associated potential-field geophysical functions are fundamentally different, and the one cannot be mapped into the other by linear transform operators. There are two problems: all the information inherent in the potential-field function can be contained in a function of two dimensions whereas the physical-property function requires three dimensions, and linear operators applied to discrete data (using, for example, discrete Fourier transforms) become unstable in the vicinity of steps. The problem of having one too many dimensions is avoided by making sufficient assumptions about the behaviour of the physical property in the extra dimension that the physical property can be completely defined by a function having the same number of dimensions as the data. The problem of discrete-data instabilities is severe. All observational data are discrete data, and consequently linear transformations such as downward continuation and susceptibility mapping commonly must rely on arbitrary band-pass filters. Linear operators cannot, in practice, deliver abrupt boundaries and do not require that the physical property be constant between physical-property domain boundaries.

The terrace-function operator

The terrace-function operator described here transforms a potential field into a step function consisting of steeps and flats (imagine rice-paddy terraces on a hillside), with the steeps located at inflection points in the original potential-field function. The operator is directly applicable to geophysical fields, such as the measured anomalous vertical component of gravitational acceleration (gravity anomalies), and therefore to scalar total intensity or other magnetic anomalies after appropriate pseudo-gravity transformation. The three-dimensional case is illustrated with aeromagnetic data, but the derivations are developed in two dimensions with synthetic gravity data for ease of presentation.

The terracing operator makes use of a window moved across the data (Fig. 1); it increases or decreases the data value at the centre of the window on the basis of the algebraic sign of the curvature. In the examples shown, the data points are equally spaced and a three-point window is used. Typically 20–40 iterations are required to produce the desired terraced effect; the operations are computationally simple and require little computer time.

$$f_{n+1}(x_o) = \begin{cases} \min f_n(x \in w), & \dfrac{\partial^2 f_n(x_o)}{\partial x^2} > 0 \\ f_n(x_o), & \dfrac{\partial^2 f_n(x_o)}{\partial x^2} = 0 \\ \max f_n(x \in w), & \dfrac{\partial^2 f_n(x_o)}{\partial x^2} < 0 \end{cases}$$

FIGURE 1

Terracing operator. Function values at data point x_o at the N+1th iteration are set to the maximum or minimum value of the function within the narrow window w (centered on x_o) on the basis of the direction of the curvature.

The output (Fig. 2) is a step function whose steeps tend to pass through the inflection points of the input function and whose flats bound local maxima and minima. In the case of input gravity data, inflection points delimit steep density boundaries and the magnitude of the anomaly is in a general sense proportional to the mass. Thus, the output terraced function can be associated with density. The association neglects gradational density variation and density variation with depth, and the units of the terraced function have no physical meaning. Even so, the terraced function provides a first approximation of a geologic-map-like physical property step function, which can be wrought into a physically meaningful model with little trouble.

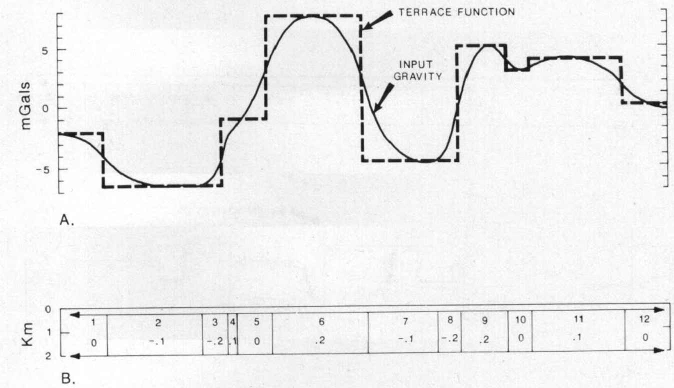

FIGURE 2

Test data. A. Input gravity profile and terraced function derived after 30 iterations. B. Model from which input gravity data was calculated, showing block numbers and relative densities (g/cm[3]). Vertical and horizontal scales are the same.

To illustrate, the gravity field (scalar vertical component, as measured in geophysical surveys) was calculated over a simple line-of-blocks model (Fig. 2-B) and is shown by the solid line in Fig. 2-A. The terraced function derived after 30 iterations is shown by the dashed line. Steeps in the terraced function exactly delineate block boundaries, with the exception of bodies four and eight. The amplitude range of the terraced function is about 14 mgal, and on the arbitrary assumption that maximum density contrast bounds would be ±0.3 g/cm^3, the terraced function was converted to a first-approximation of density contrast. The gravity field calculated from this first-approximation model (dotted line in Figs. 3-A and C) compares poorly with the original gravity field. Solving for improved density by treating these terms as ten unknowns of an over-determined linear system yielded a better fit, as shown in Fig. 3 by dashed lines. The effect of the undetected blocks four and eight is still apparent, however, in local mismatch between the calculated and original gravity fields (Figs. 3-A). A residual gravity field was obtained by subtracting the calculated from the 'observed' field and was passed a second time through the terrace function and linear inversion operation. This procedure recovered the missing blocks four and eight, and the inversion was virtually exact.

The foregoing example is intended to illustrate the procedure but is not realistic in that a one-dimensional density model within known bounds was assumed, as would not normally be possible in practice. In another case, not shown here, an input gravity anomaly was calculated for a more complicated density distribution, and the solution was constrained to a

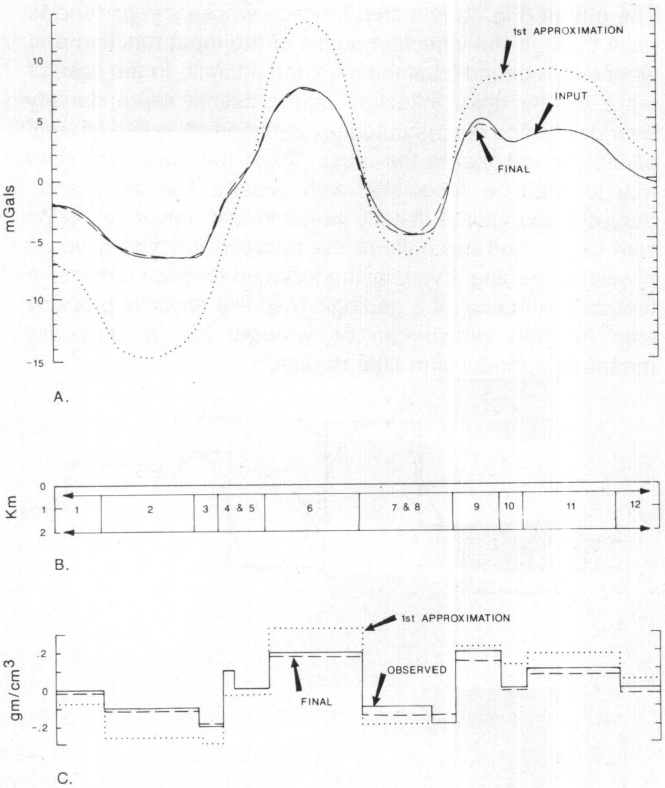

FIGURE 3
Inversion results. A. Input and calculated gravity profiles. Final results (dashed line) shown only where it departs from the input profile. B. Derived model. C. Densities of the model.

region more shallow than the model from which the input anomaly was calculated. Again, this equivalent-source model provided a reasonably good fit between calculated and input fields, which could be improved upon further by successive iterations.

Three-dimensional application

The terrace-function operator is easily extended to the three-dimensional case, allowing terraced maps to be calculated from data grids. Aeromagnetic data from a 100 by 200 km area in the central United States were transformed to pseudo-gravity, high-pass filtered to remove very long wavelengths, and terraced, Magnetic basement in this area consists of a weakly metamorphosed mid-Proterozoic terrane of granite plutons and rhyolite lavas, in part exposed, and a little-known regionally metamorphosed terrane in subsurface.

Grey-scale images of the aeromagnetic data in original and in terraced form present a striking comparison. The former shows the subtle high-frequency signature zonation characteristic of aeromagnetic images, whereas the terraced map is more like a geologic map. Major susceptibility boundaries are clearly delineated and are closely comparable with boundaries mapped independently by another objective method based on analysis of gradients. Preliminary results indicate that susceptibility-mapping via least-squares inversion of the terraced function will not differ in principle or in effectiveness from the profile case. There is, however, more labour and arbitrariness involved in defining and digitizing the domain boundaries.

Geothermal Signatures and Uranium Ore Deposits on the Stuart Shelf of South Australia

J. P. Cull
Department of Earth Sciences
Monash University
Clayton, Vic. 3168
Australia

G. A. Houseman
Research School of Earth Sciences
A.N.U., GPO Box 4
Canberra, A.C.T. 2601
Australia

P. M. Muir **H. L. Paterson**
Western Mining Corporation Ltd
Exploration Div., PO Box 57
St. Marys, S.A. 5042
Australia

Summary

The Olympic Dam copper–uranium–gold deposit coincides with a major geothermal anomaly. Excess heat flow is expressed by elevated geothermal gradients in the flat-lying Cambrian and Late Proterozoic sediments which unconformably overlie the mid-Proterozoic basement (and the ore body). The Tregolana Shale within this sequence is assumed to act as an impermeable layer in which the lateral variation of thermal conductivity is negligible. Geothermal gradients in the Tregolana Shale range from 83.6°C/km at Roxby Downs to 52 ± 8°C/km elsewhere on the Stuart Shelf. Thermal conductivities were determined in representative core samples allowing estimates of heat flow ranging from 160 to 100 mW/m^2 respectively. Most of the anomalous heat flow can be attributed to the radiogenic decay of uranium